Mapping Geologic Structures from Gravity and Digital Elevation Model in the Ziway-Shala Lakes Basin; central Main Ethiopian Rift

Hailemichael Kebede (hailekebede1995@gmail.com)
Addis Ababa University College of Natural Sciences https://orcid.org/0000-0002-0488-9340
Abera Alemu
Addis Ababa University College of Natural Sciences
Dessie Nedaw
Addis Ababa University College of Natural Sciences

Full paper

Keywords: Surface and subsurface geologic structures, lineament analysis, gravity lineaments, topographic lineament, derivative filters, upward continuation, Line module algorithm, line density histogram

Posted Date: May 29th, 2020

DOI: https://doi.org/10.21203/rs.3.rs-30871/v1

Version of Record: A version of this preprint was published at Heliyon on December 1st, 2021. See the published version at https://doi.org/10.1016/j.heliyon.2021.e08604.

Mapping Geologic Structures from Gravity and Digital Elevation Model in the Ziway-Shala Lakes Basin; central Main Ethiopian Rift

Hailemichael Kebede[1*], Abera Alemu[1] , Dessie Nedaw[1]

[1]School of Earth Science, Addis Ababa University, P.O. Box 1176, Addis Ababa, Ethiopia

[*]Corresponding author: E-mail: hailekebede1995@gmail.com

Keywords: Surface and subsurface geologic structures, lineament analysis, gravity lineaments, topographic lineament, derivative filters, upward continuation, Line module algorithm, line density histogram

Abstract

This study attempts to delineate subsurface lineaments for the tectonically and volcanically active region of the Ziway-Shala Lakes basin, central Main Ethiopian rift. Most of the previously mapped subsurface structures in the region under consideration focus on delineating crustal structures thicknesses and Moho depths undulations. Moreover, near-surface structures in the same region were mapped using analysis of Digital Elevation Model image data. On the other hand, there are few studies that have targeted in mapping geologic structures lying at intermediate depth levels between the shallower and deeper Earth. The objective of this research is thus to map the subsurface geologic structures/lineaments to an average depth of 3 km (crystalline basement layer depth) from surface using gravity data. These investigation results are validated by Digital Elevation Model extracted lineaments. Filtering techniques including derivative filters, upward-continuation and line module algorithm of PCI Geomatica are used to extract the gravity and topographic lineaments of the region. Orientation analyses of these subsurface and surface lineaments are made using line direction histogram of the QGIS software. Accordingly, the gravity subsurface lineaments mapped in this study are found to be dominantly oriented in the NNW-SSE to NW-SE and E-W direction on average. These results appear to be contrary to the NNE-SSW to NE-SW trending surface geologic structure mapped on the bases of actual field observation carried out by previous researchers and automatically extracted lineaments based on Digital Elevation Models data considered in this research. The subsurface lineaments mapped using gravity data coincide with the orientation of pre-existing subsurface structures crossing the rift orthogonally. These structural lineaments which are considered to be masked in the subsurface coincide with the orientation of the Mesozoic Ogaden rift as compared to the overlying surface structures which appear to coincide with the orientation of the Cenozoic Main Ethiopian rift.

1. Introduction

The Main Ethiopian Rift (MER) encompassing three segments, southern, central and northern MER (Woldegabriel et al., 1990) (Bonini et al., 2005) is part of a bigger East African Rift system (EARS) that links the Afar triple junction and the Kenya Rift regions. The study area, Ziway-Shala Lakes basin, is located in the central part of the Main Ethiopian rift (Ayenew, 2001) and is bounded within the limits of $38^0$00'-$39^0$30'E and $7^0$00'-$8^0$30'N. The region is characterized by volcano-tectonic depressions having three physiographic features, the rift floor and the flanking escarpments and plateaus. The mean elevation varies from 1632 masl to 3448 masl (Figure 1).

1.1 Geologic and structural settings

These geology and geologic structures observed in the region are due to the active Cenozoic volcanic, tectonic and sedimentation processes (Abebe et al., 2007; Woldegabriel et al., 2000; Le Turdu et al., 1999). These structures could be faults, joints and fractures which have surface expression as shown in the geologic map (Figure 2) and structural map (Figure 3) of the area. These structures could constitute faults, joints and fractures with their surface expression shown in (Figure 2) and (Figure 3). These surface structures generally have N-S to NNE-SSW and NE-SW to N-S (Korme et al., 2004) orientation and are collectively called Wonji Fault Belt (WFB) (Mohor, 1962) and boundary faults (Boccaletti et al., 1998). The WFB is the youngest and most active fault system cross-cut by the pre-existing NW-SE Mesozoic Ogaden rift fault (Korme et al., 2004). These pre-existing structures have been proven to exert a significant control on the accommodation of deformation and on the distribution of strong volcanic activity (Corti et al., 2013; Abebe et al., 2007) in the region.

1.2 Rationale and objective of the study

The geological structures in the East Africa Rift system documented in different literatures mainly target on extracting the surface structures of shallow Earth origin (e.g., Molin and Corti, 2015; Agostini et al., 2011). The data used to trace these surface structures are Digital Elevation Model (DEM) images. The surface structures in the Ziway-Shala Lakes basin mapped using DEM data and actual field observations (Agostini et al., 2011) is shown in Figure 2. The subsurface structures of deeper origin for the same region are extracted from geophysical data (mainly gravity and seismic), most of which focus on mapping crustal structures thicknesses and Moho depth undulations. Based on gravity data, different researches arrived at the conclusion that the crust thins northward along the rift (Mickus, 2007; Tiberi et al., 2005; Tessema and Antoine, 2004; Mahatsente et al., 1999). Refraction/wide-angle seismic reflection survey conducted along the rift (Maguire et al., 2006) support the results from gravity data. Though, its depth extent is not mentioned Korme et al. (2004) identified a pre-existing NW-SE extending Mesozoic Ogaden rift fault from gravity data. These structures cross the main Ethiopian rift in an approximately orthogonal fashion (Korme et al., 2004). In this respect, there is lack of studies that have targeted on delineating the intermediate depth (between shallower and deeper earth) geological structures at different depth levels in the Ziway-Shala Lakes basin.

By taking into consideration all the points mentioned, the objectives of this study are thus defined:

1. To map the subsurface geologic structures/lineaments to a depth of the crystalline basement (3km) using gravity data

2. To map surface structures (topographic lineaments) from DEM data and use this information to validate(constrain) the subsurface structures mapped using the gravity data.

2. Data

Gravity and Digital Elevation Model (DEM) data sets are examined for subsurface and surface structures beneath the Ziway-Shala Lakes basin, central Main Ethiopian Rift. The data acquisition and processing is documented as follows

2.1 Gravity Data

Ground based gravity data were obtained from Geological Survey of Ethiopia and PhD thesis work (Alemu, 1992). This data were reprocessed and homogenized to the International Gravity Standardization Network 1971 (IGSN71). The 1967 international gravity formula, a reduction density of 2.67 g/cm^3 and sea level as a datum are used. The computed complete Bouguer anomaly values are gridded to generate the complete Bouguer anomaly map (Figure 4(b)) of the study area. The regional anomaly is estimated using upward continuation filter with an upward continuation height of 6 km (Kebede et al., 2020) (Figure 4(c)). The residual anomaly map (Figure 4(d)) of the region is then compiled by subtracting the estimated regional from the observed complete Bouguer anomaly.

The residual anomaly map (Figure 4(d)) is characterized by negative and positive anomaly values which are subjected for further analysis to extract the shallow subsurface structures (lineaments) of the study area.

2.2 **Digital Elevation Model (DEMs)**

Digital Elevation Model (DEM) is an Advanced Space-borne Thermal Emission and Reflection Radiometer (ASTER) gridded imagery data used to represent elevation information of the study area from which surface geologic structures are mapped from. The DEM data employed here has a 30 m spatial resolution (Figure 5).

According to Wladis (1999) since DEM data is a gridded data, grid-based interpretation methods used in analysis of potential field data can be used to extract surface lineaments for a region of interest.

3. Methodology

Mapping surface and subsurface structures based on DEM and potential field data is a well practiced and established procedure. Contacts between rocks that have different physical properties usually occur along weak boundaries (lineaments) which may consist of faults fractures, etc. Such lineaments which could show major subsurface structures are extracted using image filtering algorithms applied on gravity anomaly data (Aydogan, 2011; Saibi et al., 2008). Topographic lineaments (Kassou et al., 2012; Abdullah et al., 2010; Jordan et al., 2005; Wladis, 1999) are traced from DEM data using the same filtering techniques used in the analysis of gravity data.

In this research the filter types used include first vertical derivative, second vertical derivative, tilt derivative, upward continuation and line module algorithm of PCI Geomatica. The application of these filters on gridded image map help to extract information on surface and subsurface structures of the area. The governing mathematical equations for the filter types considered are described below

3.1 First and second vertical derivative

Vertical derivatives (VDR) are data filtering techniques used for the enhancement of the shallow gravity source features. Gridded gravity and DEM anomaly data input to VDR filters can be expressed as a function in Cartesian co-ordinate system denoted by $F = f(x, y, z)$.

The vertical derivatives of this function which shows the change of field/elevation with respect to depth (z) is expressed as first vertical derivative $(FVDR)$ (Eq. 1):

$$FVDR = -\frac{\partial f}{\partial z} \tag{1}$$

and second vertical derivative $(SVDR)$ (Eq. 2):

$$SVDR = -\frac{\partial^2 f}{\partial z^2} \tag{2}$$

The Oasis montaj Geosoft standard software is used to generate the first and second order derivatives of the gridded DEM image. The procedures have effects of enhancing localized shallow (near surface) sources and generate lineaments.

3.2 Tilt derivative

The tilt derivative (θ) of gravity anomaly, **F**, is expressed as a ratio of its first vertical derivative to total horizontal derivative (Verduzco et al., 2004) (Eq. 3):

$$\theta = TDR = tan^{-1} \frac{\frac{\partial F}{\partial z}}{\sqrt{\left(\frac{\partial F}{\partial x}\right)^2 + \left(\frac{\partial F}{\partial y}\right)^2}} \tag{3}$$

Where, $\frac{\partial F}{\partial x}, \frac{\partial F}{\partial y}$ and $\frac{\partial F}{\partial z}$ are the derivatives of the gravity anomaly, **F,** with respect to x, y *and* z directions.

A mathematical property of arctan restricts the value of θ to lie between $-\frac{\pi}{2}$ and $-\frac{\pi}{2}$ or between -90^0 and 90^0.

The filter enhances and sharpens the anomalies with zero value contours (zero crossing) which indicate lithological /structural contacts.

3.3 Upward continuation

Vertical derivative and tilt derivative filters generally enhance effect of the shallower earth but not necessarily effect of the deeper earth. The regional anomaly resulting from the deeper earth is approximated using the upward continuation filter which is mathematically expressed by Gupta and Ramani (1980) and Jacobsen (1987) (Eq. 4) as:

$$H_{reg}(k) = S_0(k)\, e^{-2\pi k z_0} \tag{4}$$

Where $S_0(k)$ is Bouguer anomaly, k is the wave number and $\boldsymbol{z_0}$ is the continuation height

The deeper gravity source signatures are isolated by upward continuing the observed Bouguer anomalies to a higher elevation. According to Jacobsen (1987), if a potential field is upward continued to a certain height, Z, then it will map sources situated at and below the depth $Z/2$. The residual anomaly is then obtained through subtraction of this regional anomaly from the observed Bouguer anomalies.

Jacobsen (1987) also showed that the field generated by a slab located at depths in between Z_1 and Z_2 is simply the difference between the fields resulting from upward continued heights of $2Z_1$ *and* $2Z_2$ (Figure 6).

The following procedures are followed for the extraction of lineaments emanating from a sandwiched (sliced) gravity source distribution (Figure 6).

- ✓ upward continuation of the observed Bouguer anomaly to a heights of 0.5, 1, 2, 3, 4, 5 and 6 kms
- ✓ Obtaining differences of consequently upward continued anomalies to generate anomalies originating from slabs (slices) located at consecutive depths between 0.25 & 0.5, 0.5 and 1, 1 and 1.5, 1.5 and 2, 2 and 2.5, 2.5 and 3.0, 1.5 and 3km.
- ✓ For anomalies resulting from each slice, line module algorithm of PCI Geomatica and tilt derivative filters are applied to extract lineaments resulting from each slice.

The Bouguer gravity anomaly map (Figure 4(a)) is upward continued to heights of 0.5, 1, 2, 3, 4, 5 and 6 km in order to image sources buried at depths of 0.25, 0.5, 1, 1.5,2, 2.5 and 3.0 km respectively. This upward continuation filter (low-pass filter) generates regional anomalies subtracted from each other giving rise to regional anomalies generated by slabs (sliced slabs) located at depths between 0.25 & 0.5, 0.5 & 1, 1 & 1.5, 1.5 & 2, 2 & 2.5 , 2.5 & 3.0 and 1.5 & 3 km. As an illustration, the anomalies generated by sliced slabs between the depths 0.25 & 0.5 km, 1.5 & 2 and 2.5 and 3 km are depicted in Figure 7(a), Figure 7(b) and Figure 7(c).

Oasis Montaj Geosoft is used to filter the regional anomalies generated by sliced slabs located at the depths considered and PCI Geomatica software is used to extract the geologic lineaments occurring in the area to a depth of 3 km (≈ mean crystalline basement depth). The differenced regional anomalies (anomalies of the sliced slabs) are exported as shaded-relief Geotiff 256 Grey (8 bit) images to be used as an input to the Line module algorithm of PCI Geomatica V10. The exported images emphasize gradients in anomaly grids and are useful for displaying strong linear features

observed in the images. The methods automatically identify lineation in three steps including edge detection, thresholding and curve extraction (details given in section 3.4).

3.4 Line module Algorithm

The LINE option of PCI Geomatica software extracts lineaments automatically from images and records the polylines in a vector segment (Abdullah et al., 2010). This algorithm is designed to extract linear and curvi-linear features from radar images or from optical images. For mapping reasonably acceptable lineaments, the images should be enhanced with different filtering techniques which may include shaded-relief methods performed using ArcGIS 10.3 software or principal component analysis (PCA) method performed using Image processing software such as ENVI 5.1. The PCA is a statistical technique which removes data redundancy and isolates noises by enhancing images which could finally be used as an input to the filters for extracting geological lineaments (Adiri et al., 2016).

The other image enhancement method is the shaded-relief image techniques which generate a pan sharpened 8 bit gray scale reflected bands to be used as input to Line module of PCI Geomatica V10 software to automatically extract geological lineaments. This algorithm detects the lineation in three steps which include edge detection step, thresholding step and curve extraction step. The input output parameters pertaining to this algorithm including their relationship can be found in the website http://www.pcigeomatics.com/geomatica-help/references/pciFunction_r/python/P_line.html.

The optimal choice of the input/output parameters is chosen by a trial and error process with the shape and density of the generated lineaments taken in to consideration. The default input parameters used by PCI Geomatica algorithm including the selections made in this research are listed in Table 1.

Mapping geological structures (lineaments) of intermediate depth in the region considered are performed using different software such as Geosoft, ENVI 5.1, PCI Geomatica V10, ArcGIS 10.3 and QGIS.

4 Results and Discussion

Geologic structures which could be faults, fractures and joints can be extracted from analysis of gravity and DEM data. The application of different filtering algorithms on these anomalies/images generates gravity and topographic lineaments outlined here below.

4.1 Subsurface lineaments extraction from gravity slice anomalies

Figure 8 reveals gravity lineaments extracted in the study area based on the methodologies mentioned in sections 3.2, 3.3 and 3.4. These includes lineaments extracted based on Line module algorithm (Figure 8 (a, c and e)), tilt derivative techniques (Figure 8 (b, d and f)) and rose diagram plot showing the overall subsurface lineaments orientation constructed based on line direction histogram module of QGIS (Figure 8(g))

The major geological structures (lineaments) (Figure 8) which are seen in the form of linear geometries are extracted through analyzing gravity data. The line module algorithm of PCI Geomatica is used to extract these lineaments (Figure 8 (a), (c) and (e)). These lineaments are compared with lineaments mapped using the tilt derivative method (Figure 8 (b), (d) and (f)). Their comparison shows that both methods give similar results in identifying the location, orientation and density of lineaments in the study area. The extracted lineaments are dominantly oriented NNW-SSE to NW-SE and E-W (Figure 8(g)) which thought to coincide with the direction of pre-existing Mesozoic structures previously identified in the area (Korme et al., 2004). The result also shows lineaments trending NE-SW (Figure 8(g)) that coincides with the orientation of the quaternary faults of the Main Ethiopian Rift system that comprises the study area.

The subsurface lineaments can also be extracted from residual gravity anomalies at different depth levels. The estimated regional anomalies generated using upward continuation to heights of 0.5, 1, 2, 3, 4, 5 and 6 km are subtracted from observed Bouguer anomaly to extract residual anomalies caused by sources extending to depths of 0.25 km, 0.5 km, 1.0 km, 1.5 km, 2.5 km and 3.0 km respectively. These residual anomalies are then converted to 8 bit shaded relief images to be used as an input to line module algorithm which help to extract subsurface lineaments at different depth levels. The identified lineaments (Figure 9 (a), (b), (c), (d), (e) and (f)) are dominantly oriented in a NW-SE direction as also revealed by the rose diagram plot (Figure 9(g)). These linear features (lineaments) are in agreement with respect to their location, orientation and density with those lineaments extracted based on the regional gravity anomalies caused by sliced slabs (Figure 8).

4.2 Surface Lineaments extracted from DEM

The topographic lineaments considered in this section are traced using the procedure and methods outlined in sections 3.1 and 3. 4.

4.2.1 First and second vertical derivative

The application of first vertical derivative filter on DEM image map generates slope image map shown in Figure 10 (a). This map reveals surface structures coinciding with the existing Cenozoic fault patterns observed in the study area (Agostini et al., 2011). Similarly, according to Wladis (1999) the second order derivative filter was used for detection of lineaments. This method has the effect of enhancing anomalies over anomalous sources. The topographic lineaments (Figure 10(b)) mapped using this method also shows the dip directions of the structure towards blue color contrast.

Figure 10 First vertical derivatives of topographic (DEM) data (a) Lineaments extracted from DEM using second order derivative with dip directions towards low color contrast (e.g. blue color) (b)

The lineaments extracted using derivative filters (Figure 10) give clearer picture of shallow source anomalies with the linear features indicating geologic structures observed in the area. Furthermore, the linear topographic lows may be thought to indicate depressions existing in the area.

4.2.2 Line module of PCI Geomatica

Lineaments are automatically extracted using the Line module algorithm with enhanced slope image of DEM and the input parameters options as choice 1 and choice 2 indicated in Table 1 resulting in Figure 11(a) and Figure 11 (b). A lineament density map (Figure 11 (c)) is derived from the slope image lineament map (Figure 11 (a)) fed as an input to ArcGIS software.

With the default parameters (choice 0) (Table 1) in PCI Geomatica software few lineaments (faults) were mapped in the area. However, with a change of threshold edge gradient from 100 to 20 (choice 1) and all the others parameters kept constant, the program generates the lineaments shown in Figure 11 (b).

Similarly, the result based on input parameters given in choice 2 produces lineaments shown in the Figure 11 (a). These structures are all similar in orientation and location to that of lineaments traced based on choice 1. However, they are more linear in shape and shorter in size. In this case all the curved structures are wiped-out with their linearity preserved. Generally, the two parameter options chosen mostly generate lineaments of the study area. However, there is a need to experiment on the selection of the input parameters for better extraction of lineaments in the study area. The lineation density map (Figure 11 (c)) shows more lineaments on the Eastern escarpment where the WFB is located as compared to those on the Western escarpment where Silti Debre Zeyete Fault Zone (SDFZ) is located including their accompanying border faults. The extracted geological structure (lineaments) statistically analyzed (trend analyzed) and plotted in the form of rose diagrams (Figure 11(d)).

The lineaments generated with PCA enhanced DEM image (Figure 12(a)) input to the line module of Geomatica software is shown in Figure 12(b). The result shows that, the mapped

structures agree with previously identified fault maps in location, orientation and density. However, in this work more lineaments were mapped. Higher densities of lineaments are observed at WFB and SDFZ and lower density of lineaments corresponding to the sedimentary units of the rift floor Figure 12(b).

In summary, the lineaments extracted with first derivative of DEM as an input to Line module PCI Geomatica (Figure 11(a)) mostly agree with fault map (Figure 3(b)) previously mapped in the area. Most of these lineaments oriented NNE-SSW as the summery made by line density rose diagram shows (Figure 11(d)). PCA enhanced DEM input to Line module algorithm of PCI Geomatica (Figure 12(b)) equivalently map the structure with more new lineaments. In both lineament extraction procedures it is observe that too many lineaments than the true faults or tectonic features of the study area.

Most of the deep seated lineaments extracted from gravity data oriented NNW-SSE to NW-SE (Figure 8 (g) and Figure 9(g)). Few of these lineaments traced using these data trends N-S and NE-SW. Majority of the traced lineaments from DEMs image trends NNE-SSW to NE-SW and N-S (Figure 11(d)) direction which agree with few gravity lineaments in the study area (Figure 8 (g) and Figure 9(g)). This shows few surface lineaments continued down depth. Minor surface lineaments trending along NW-SE coincide with the orientation of most subsurface lineaments extracted using gravity data.

Furthermore, most surface and subsurface lineaments out of the Main rift axis in an Ethiopian plateau oriented in the direction of pre existing structural orientation (NW-SE) (Figure 12 (d)). This was also reveled by different researchers that the crust outside the rift axis in Ethiopian Plateau has not been modified significantly by Cenozoic rifting and magmatism (Dugda et al., 2005) (Gani et al., 2008).

5. Conclusion

One way of studying the geological structure of an area is through studying linear features (lineaments) which could be extracted from gridded data anomalies. In this paper gravity and Digital Elevation Model (DEMs) anomaly data are used to map the corresponding gravity and topographic lineaments of the study area. The first and second vertical derivatives; tilt derivative, upward continuation, line module algorithms are used to automatically extract lineaments in the study area. Most subsurface lineaments extracted from gravity data oriented NNW-SSE to NW-SE directions which are against most surface structural orientation (NNE-SSW to NE-SW) mapped earlier by different researchers and extracted automatically based on DEM data considered in this research. The subsurface lineaments orientation might be due to the pre-existing subsurface structures crossing the rift orthogonally while surface structures might be due to Cenozoic rifting activities. A higher surface lineament density is observed in the eastern parts of the study area than the western side. Out of the rift most of the surface lineaments are oriented NW-SE which coincides with gravity data extracted pre-existing structures that strike the MER orthogonally. It can be concluded from the result that the integration of extracted topographic lineaments (surface structures) with potential field lineaments (subsurface structures) will add some information on the enhancements of the previously extracted structural map of the area.

List of Abbreviations:

MER: The Main Ethiopian Rift

WFB: Wonji Fault Belt

SDFZ: Silti Debre Zeyete Fault Zone

DEM: Digital Elevation Model

IGSN71: International Gravity Standardization Network 1971

ASTER: Advanced Space-borne Thermal Emission and Reflection Radiometer

VDR, **FVDR, SVDR** and **TDR**: Vertical derivative, First Vertical Derivative, second Vertical Derivative and tilt derivative

PCA: Principal Component Analysis

ArcGIS: Aeronautical Reconnaissance Coverage Geographic Information System

QGIS software: Quantum Geographic Information System software

ENVI 5.1: Environment for Visualizing Images

PCI Geomatica: Remote sensing desktop software package for processing earth observation data

Declarations:

- **Availability of data and materials**

  After the completion of the PhD program (principal author), the gravity data can be requested from the authors.

- **Competing interests**

  The authors declare no conflict of interest.

- **Funding**

  This research did not receive any specific grant from funding agencies in the public, commercial, or not-for-profit sectors

- **Authors' contributions**

Dessie Nedaw

H. Kebede: Conceived and designed the experiments; Performed the experiments; Analyzed and interpreted the data; Contributed reagents, materials, analysis tools or data; Wrote the paper.

A. Alemu: Analyzed and interpreted the data; Contributed reagents, materials, analysis tools or data; Wrote the paper.

D. Nedaw: Analyzed and interpreted the data; analysis tools or data; wrote the paper.

- **Acknowledgments**

The corresponding author acknowledges Ambo University for giving a privilege to attend PhD in Geophysics. I thank Addis Ababa University for logistical support and fund for magnetic data collection. Secondary gravity data was provided by Ethiopian Geological Survey (EGS) which need to be acknowledged. No funding for analysis, interpretation of data and manuscript writing. The author would also like to thank Professors Bekele Abebe and Seifu Kebede for their critical comments to improve the manuscript. The processing were performed using Geosoft Oasis-Montaj geophysical software, ArcGIS, QGIS, ENVI 5.1 and Geomatica softwares. Finally, the author greatly appreciates all who directly or indirectly contributed to this research manuscript.

Additional information

No additional information is available for this paper.

References

Abdullah, A., Akhir, J. M., & Abdullah, I. (2010). The Extraction of Lineaments Using Slope Image Derived from Digital Elevation Model : Case Study of Sungai Lembing – Maran area , Malaysia . *Journal of Applied Sciences Research*, *6*(11), 1745–1751.

Adiri, Z., El Harti, A., Jellouli, A., Maacha, L., & Bachaoui, E. M. (2016). Lithological mapping using Landsat 8 OLI and Terra ASTER multispectral data in the Bas Drâa inlier, Moroccan Anti Atlas. *Journal of Applied Remote Sensing*, *10*(2), 025013. https://doi.org/https://doi.org/10.1117/1.JRS.10

Agostini, A., Bonini, M., Corti, G., Sani, F., & Manetti, P. (2011). Distribution of Quaternary deformation in the central Main Ethiopian Rift, East Africa. *Tectonics*, *30*(4), 1–21. https://doi.org/10.1029/2010TC002833

Alemu, A. (1992). The Gravity Field and Crustal Structure of the Main Ethiopian Rift. Ph.D. Thesis, Royal Institute of Technology, Department of Geodesy, Report No. 26 (TRITA GEOD 1026), Stockholm, Sweden.

Aydogan, D. (2011). Extraction of lineaments from gravity anomaly maps using the gradient calculation : Application to Central Anatolia. *Earth Planets Space*, *63*, 903–913. https://doi.org/10.5047/eps.2011.04.003

Ayenew, T. (2001). Numerical Groundwater flow Modeling of the Central Main Ethiopian rift Lakes basin. *SINET: Ethiopian Journal of Science*, *24(2)*(ISSN:0379-2897), 167–184.

Boccaletti, M., Bonini, M., Mazzuoli, R., Abebe, B., Piccardi, L., & Tortorici, L. (1998). Quatemary oblique extensional tectonics in the Ethiopian Rift (Horn of Africa) ,. *Tectonophysics*, *287*, 97–116.

Bonini, M., Corti, G., Innocenti, F., Manetti, P., Mazzarini, F., Abebe, T., & Pecskay, Z. (2005). Evolution of the Main Ethiopian Rift in the frame of Afar and Kenya rifts propagation Evolution of the Main Ethiopian Rift in the frame of Afar and Kenya rifts propagation.

TECTONICS, 24. https://doi.org/10.1029/2004TC001680

Corti, G., Sani, F., Philippon, M., Sokoutis, D., Willingshofer, E., & Molin, P. (2013). Quaternary volcano-tectonic activity in the Soddo region , western margin of the Southern Main Ethiopian Rift. *Tectonics*, *32*, 861–879. https://doi.org/10.1002/tect.20052

Dugda, M. T., Nyblade, A. A., Julia, J., Langston, C. A., Ammon, C. J., & Simiyu, S. (2005). Crustal structure in Ethiopia and Kenya from receiver function analysis : Implications for rift development in eastern Africa. *Journal of Geophysical Research*, *110*, B01303. https://doi.org/10.1029/2004JB003065

Gani, N. D., ABDELSALAM, M. G., GERA, S., & GANI, M. R. (2008). Stratigraphic and structural evolution of the Blue Nile Basin, Northwestern Ethiopian Plateau. *Geological Journal*, *43*, 487–510. https://doi.org/10.1002/gj

Gupta, V. K., & Ramani, N. (1980). Some aspects of regional- residual separation of gravity anomalies in a Precambrian terrain. *Geophysics*, *45*(9), 1412–1426. https://doi.org/10.1190/1.1441130

Jacobsen, B. H. (1987). Case for Upward Continuation As a Standard Separation Filter for Potential-Field Maps. *Geophysics*, *52*(8), 1138–1148. https://doi.org/10.1190/1.1442378

Jordan, G., Meijninger, B. M. L., & Hinsbergen, D. J. J. Van. (2005). Extraction of morphotectonic features from DEMs : Development and applications for study areas in Hungary and NW Greece. *International Journal of Applied Earth Observation and Geoinformation 7*, *7*, 163–182. https://doi.org/10.1016/j.jag.2005.03.003

Korme, T., Acocella, V., & Abebe, B. (2004). The Role of Pre-existing Structures in the Origin,

Propagation and Architecture of Faults in the Main Ethiopian Rift. *Gondwana Research*, *7*(2), 467–479.

Maguire, P. K. H., Keller, G. R., Klemperer, S. L., Mackenzie, G. D., Keranen, K., Harder, S., et al. (2006). Crustal structure of the northern Main Ethiopian Rift from the EAGLE controlled-source survey ; a snapshot of incipient lithospheric break-up. *The Geological Society of London*, 269–291.

Mahatsente, R., Jentzsch, G., & Jahr, T. (1999). Crustal structure of the Main Ethiopian Rift from gravity data : 3-dimensional modeling. *Tectonophysics*, *313*, 363–382.

Mohor, P. (1962). *The Ethiopian Rift System*. Bull. Geophys. Observ., Addis Ababa, 5, 33–62.

Molin, P., & Corti, G. (2015). Topography, river network and recent fault activity at the margins of the Central Main Ethiopian Rift (East Africa). *Tectonophysics*, *664*, 67–82. https://doi.org/10.1016/j.tecto.2015.08.045

Saibi, H., Nishijima, J., Hirano, T., Fujimitsu, Y., & Ehara, S. (2008). Relation between structure and low-temperature geothermal systems in Fukuoka city , southwestern Japan. *Earth Planets Space*, *60,* 821–826.

Tefera, M., Chernet, T., & Haro, W. (1996). Geology of Ethiopia. *Geological Survey of Ethiopia*. Retrieved from www.gse.gov.et/index.php/geology-of-ethiopia

Le Turdu, C., Tiercelin, J. jacques, Gibert, E., Travi, Y., Lezzar, K. E., Richert, J. P., et al. (1999). The Ziway – Shala lake basin system , Main Ethiopian Rift : Influence of volcanism , tectonics , and climatic forcing on basin formation and sedimentation. *Palaeogeography, Palaeoclimatology, Palaeoecology*, *150*, 135–177.

Verduzco, B., Fairhead, J. D., Green, C. M., & Mackenzie, C. (2004). New insights into magnetic derivatives for structural mapping. *Leading Edge*, (13), 116–119.

Wladis, D. (1999). Automatic Lineament Detection Using Digital Elevation Models with Second Derivative Filters. *Photogrammetric Engineering & Remote Sensing*, *65*(4), 453–458.

Woldegabriel, G., Aronson, J., & Walter, R. C. (1990). Geology , geochronology , and rift basin development in the central sector of the Main Ethiopian Rift. *Geological Society of America Bulletin*, *102*, 439–458. https://doi.org/10.1130/0016-7606(1990)102<0439

Figures

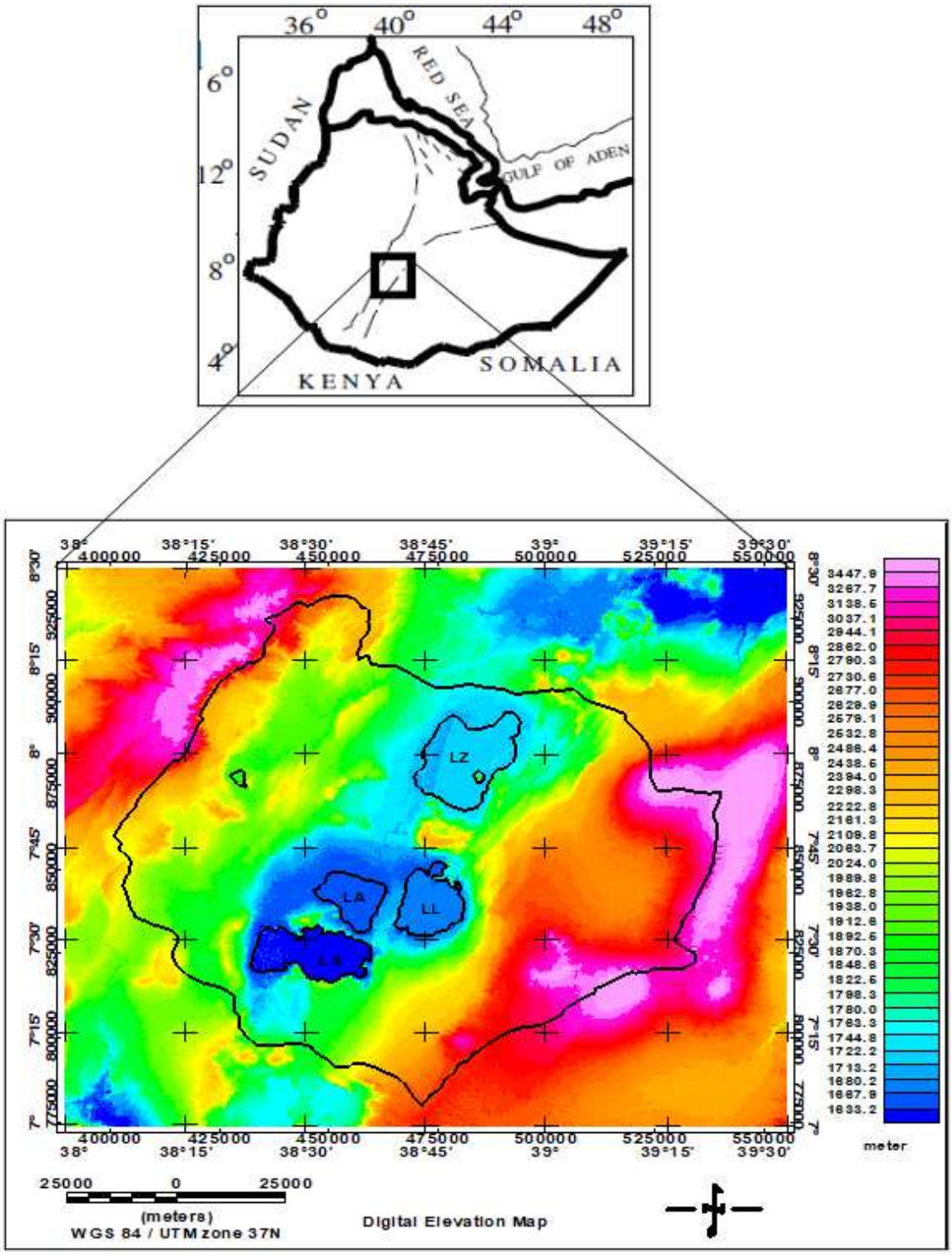

Figure 1

Location and topographic map of the Ziway-Shala lakes basin and its surroundings with the main physiographic elements

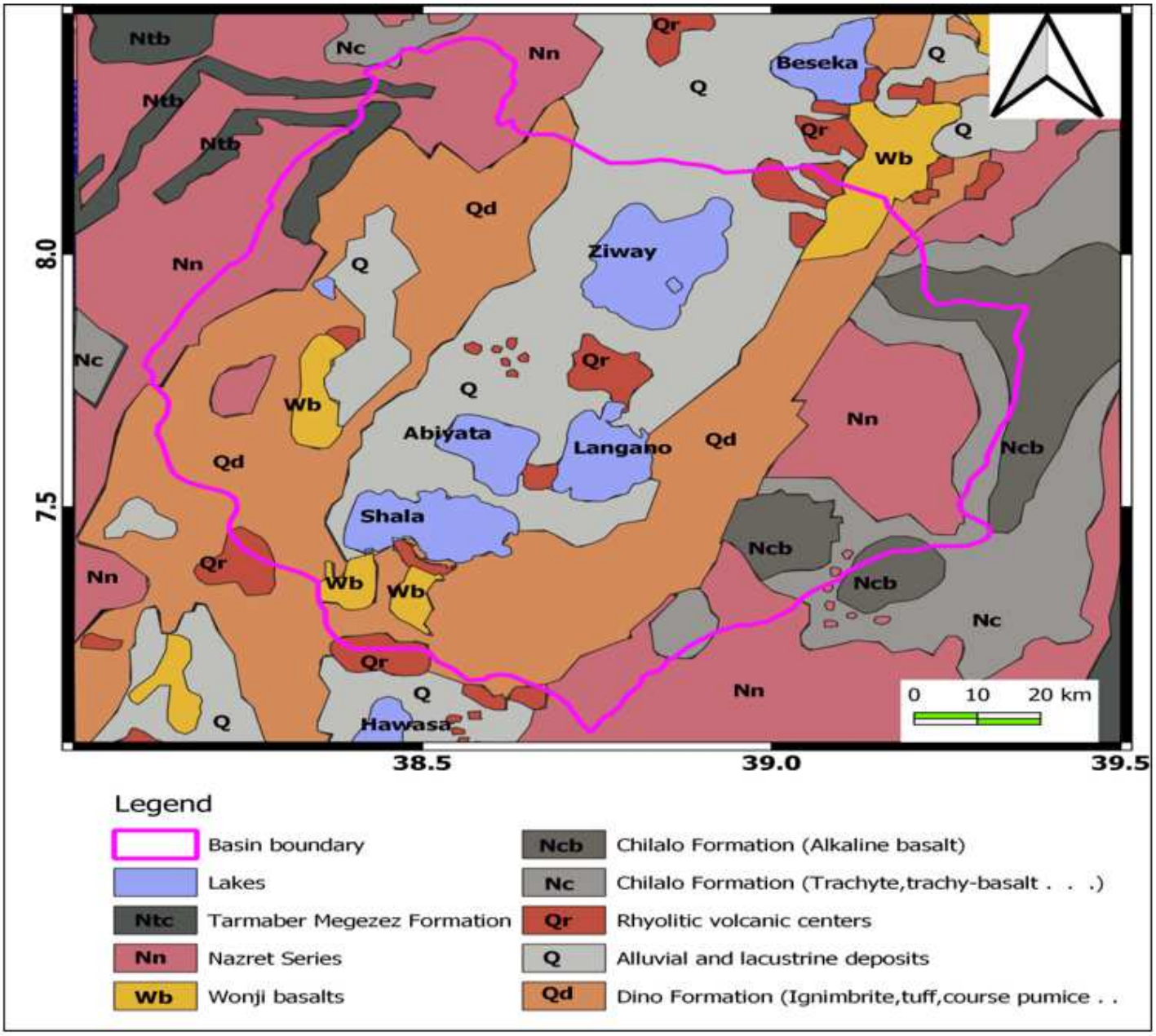

Figure 2

Geology of the Ziway-Shala Lakes basin, central Main Ethiopian rift modified from Tefera et al.(1996)

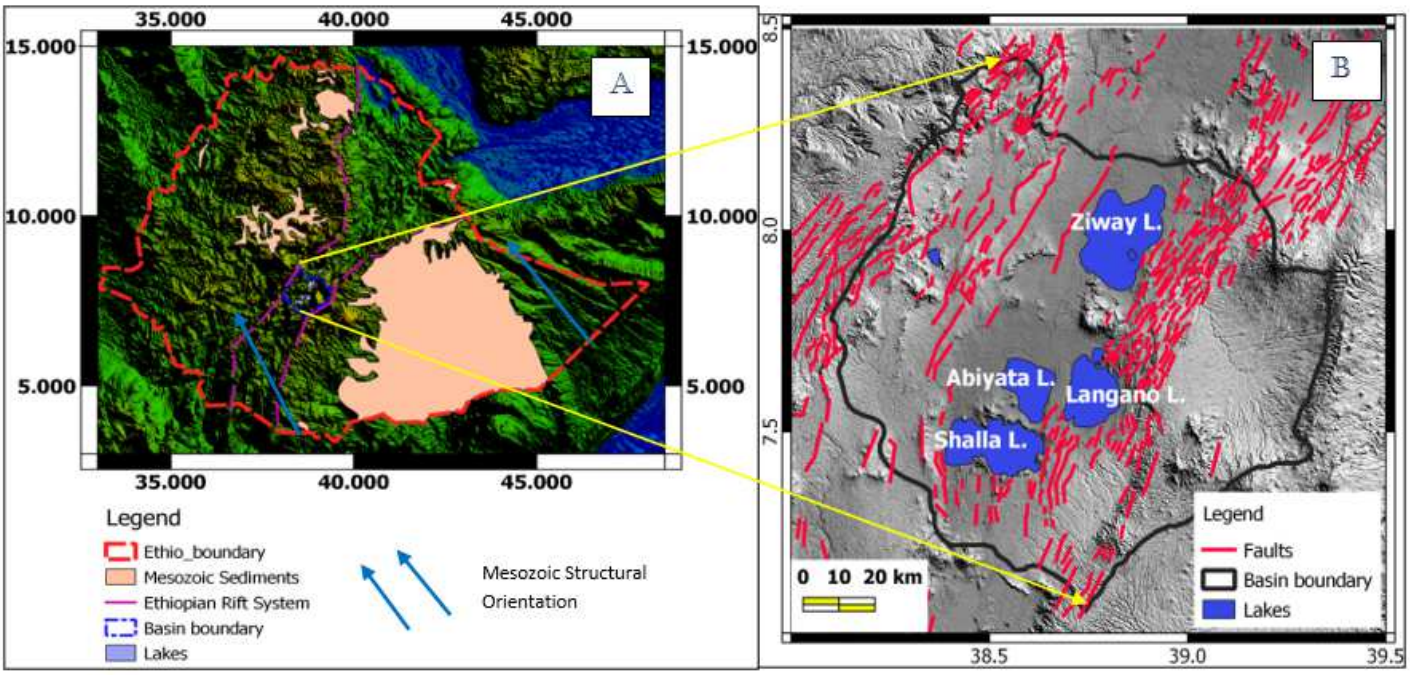

Figure 3

Outcropped Mezozoic structural orientaion which is called pre-existing Mesozoic structures (a) Surface structural map of the study area modified from Agostini et al.(2011) and Molin and Corti (2015)

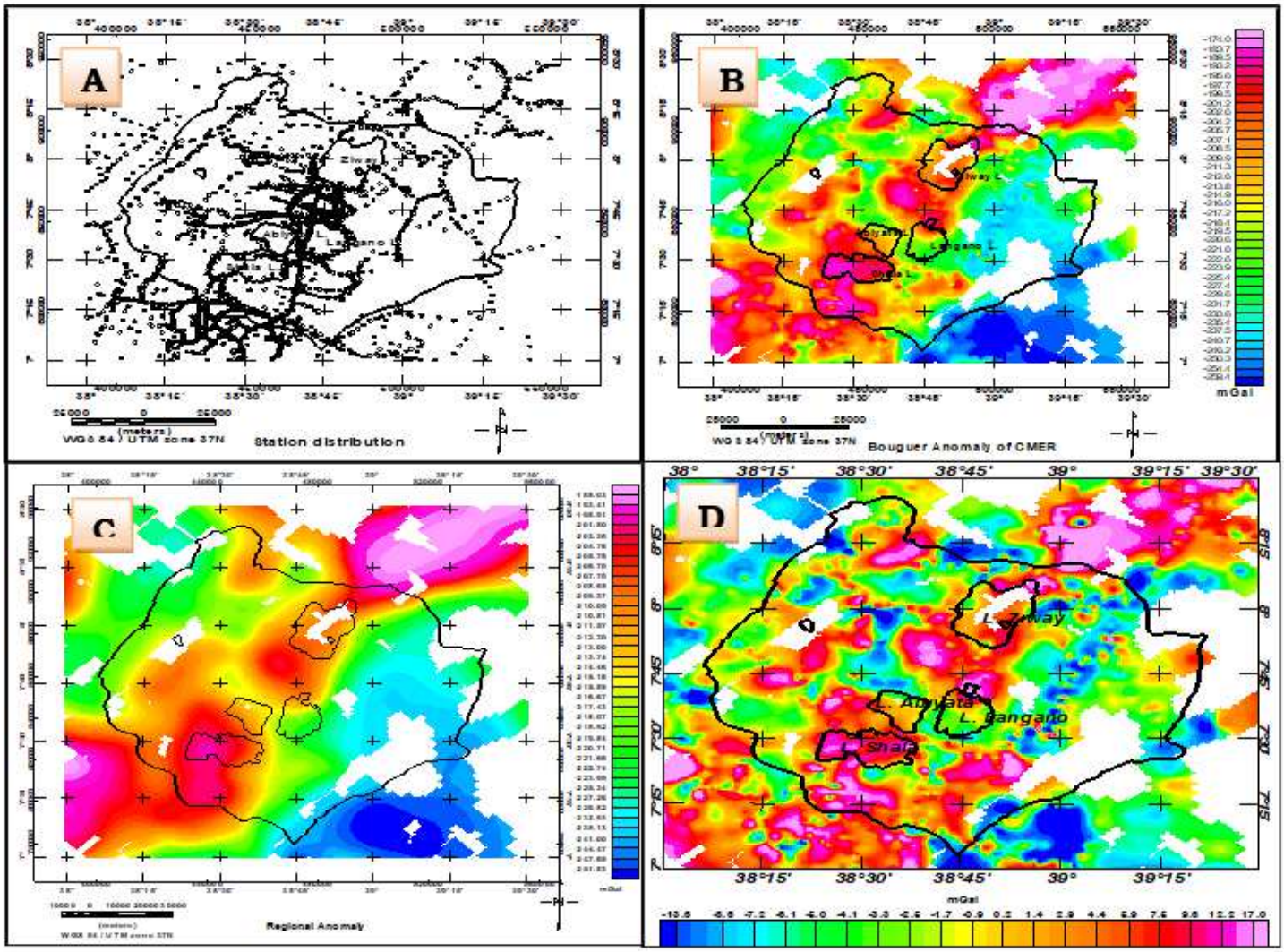

Figure 4

Gravity stations distribution map (a) Bouguer anomaly map (b) regional anomaly map (c) and residual anomaly map (d)

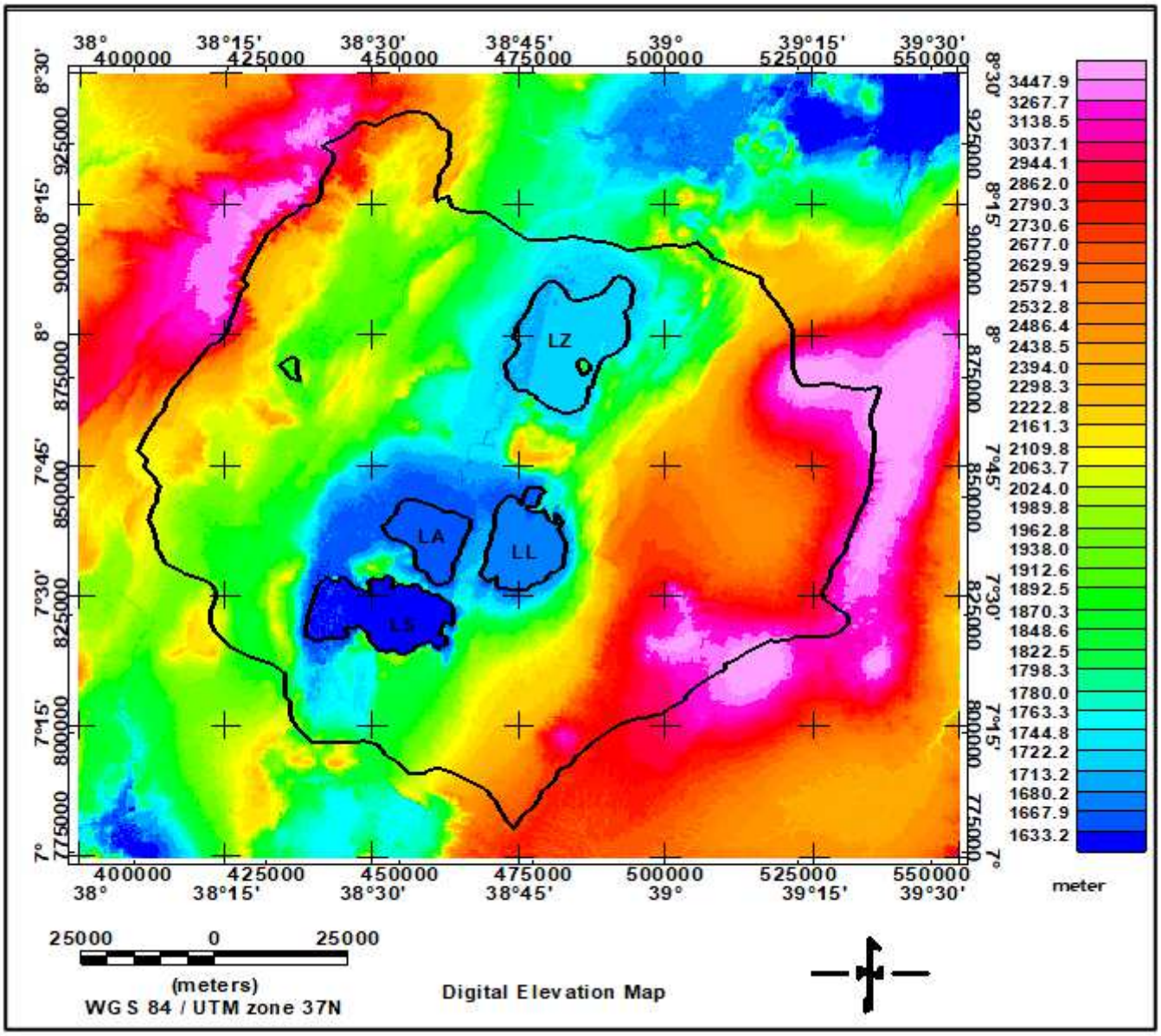

Figure 5

Digital Elevation model (DEMs) of the Ziway-Shala lakes basin and its surroundings

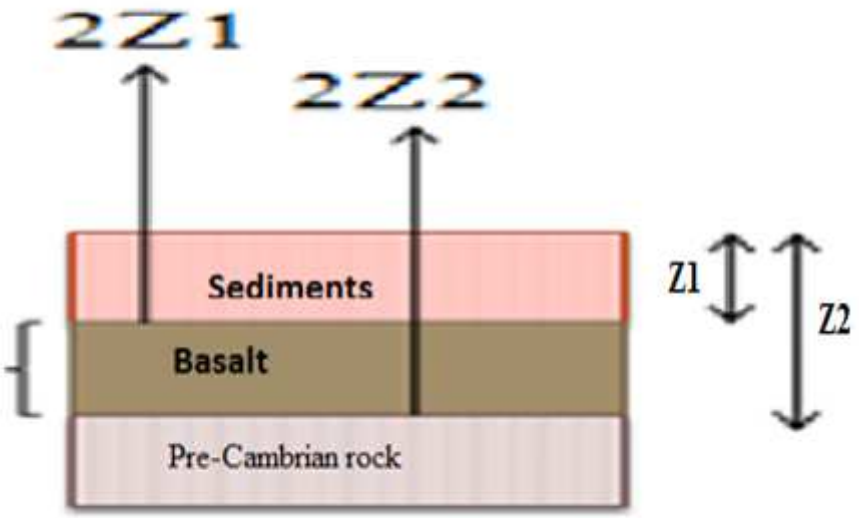

Figure 6

Schematic representation of three earth layers for extraction of the gravity field anomaly response of a slab (eg. basaltic rock formation) located between depths Z1 and Z2 by upward continuation to heights of 2Z_1 and 2Z_2

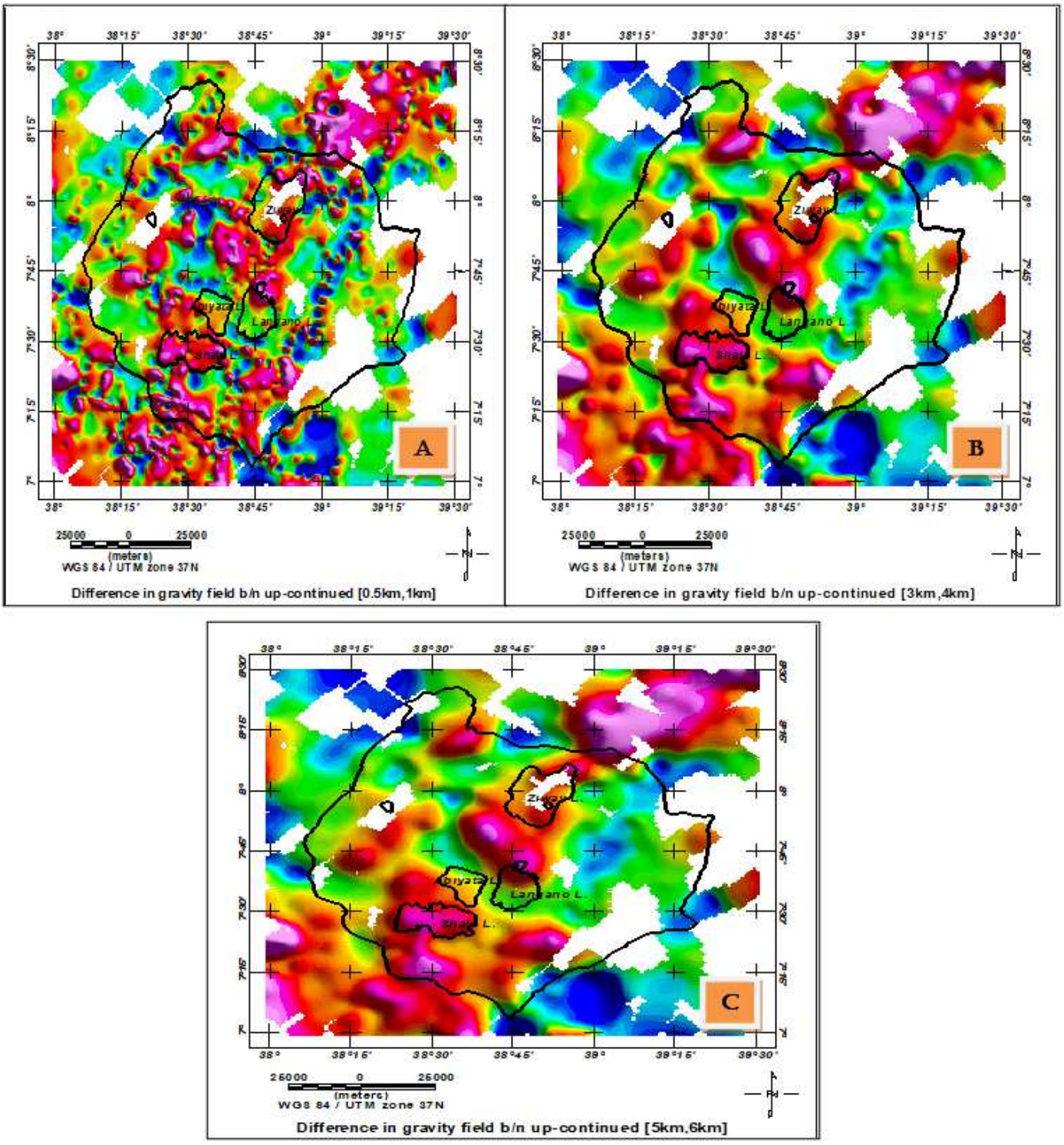

Figure 7

The gravity anomaly maps of sources (sliced slabs) compiled by taking the differences in up-continued gravity field between 0.5km and 1km (a) 3 km and 4km (b) 5 km and 6 km (c)

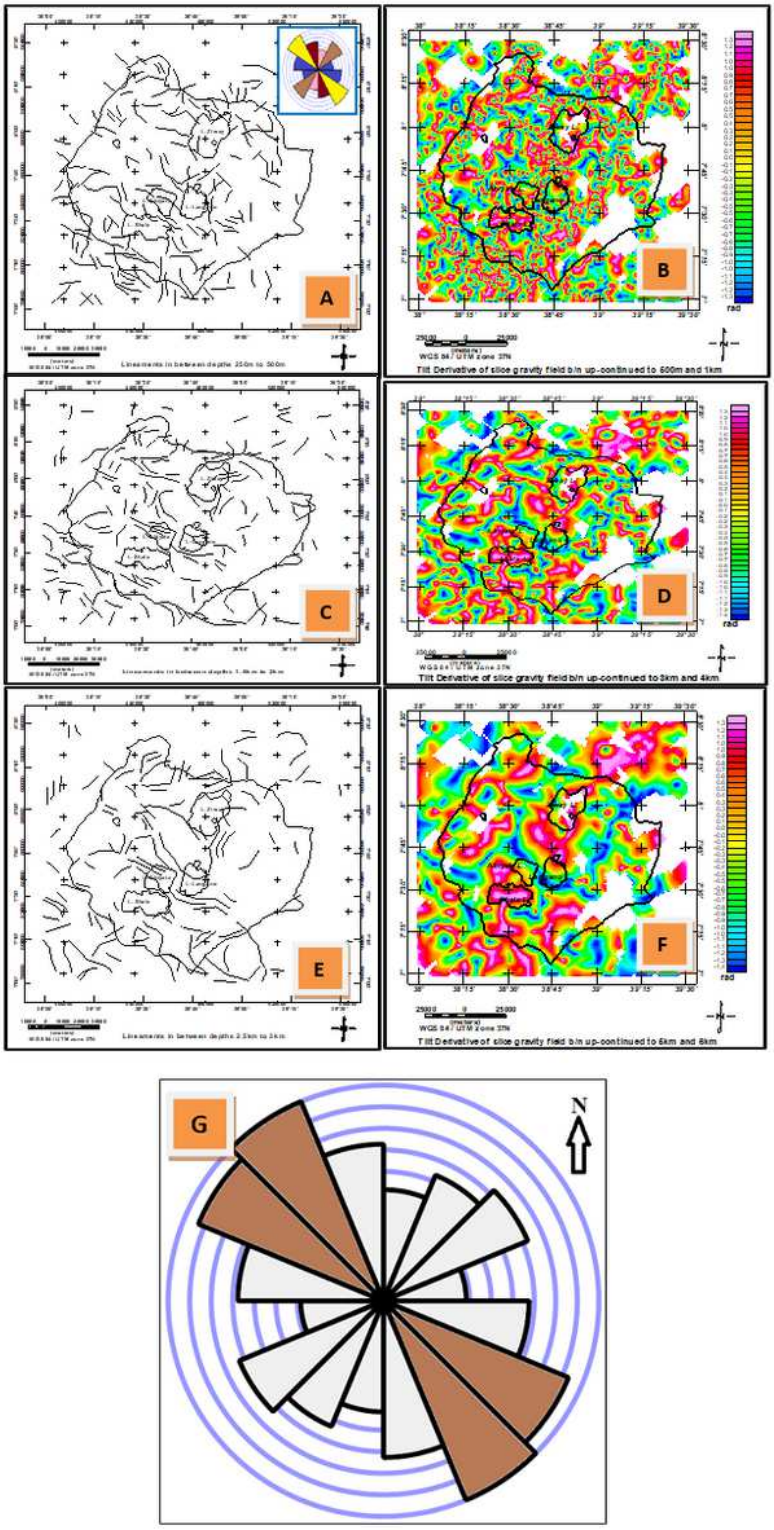

Figure 8

Lineament maps (a), (c) and (e) for depths between 250m and 500m, 1.5 and 2.0; 1.5 and 2.5 and 3km respectively compared with lineament maps generated using tilt derivative (b), (d) and (f) and rose diagram plot (g) showing orientations of the subsurface lineaments (g)

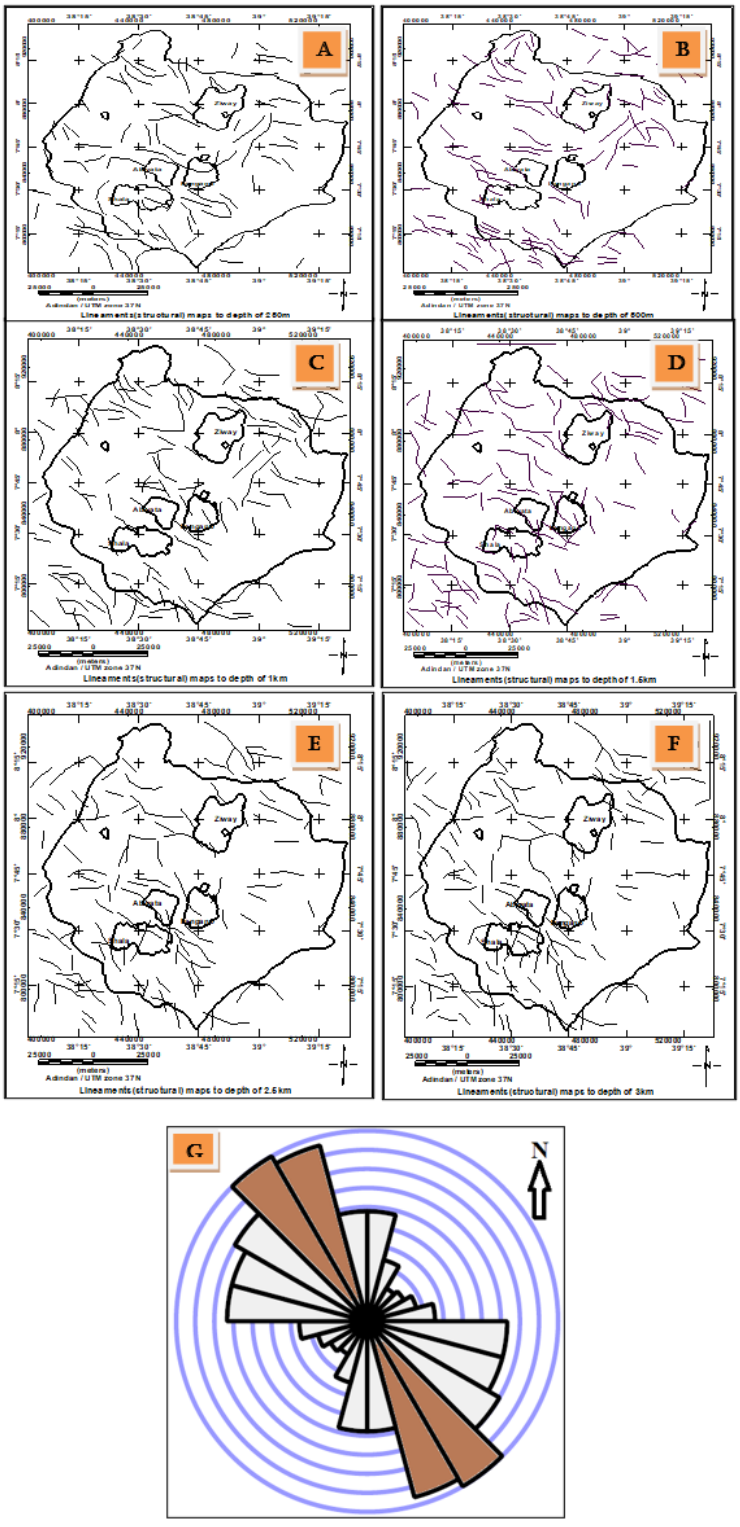

Figure 9

Lineaments maps extracted from the residual gravity anomaly map to depths of 0.25km (a), depth of 0.50 km(b), to depth of 1.0 km (c), to depth of 1.5 km (d), to depth of 2.5 km (e) and to depth of 3.0 km (f) rose diagram plot showing orientations of the subsurface lineaments (g)

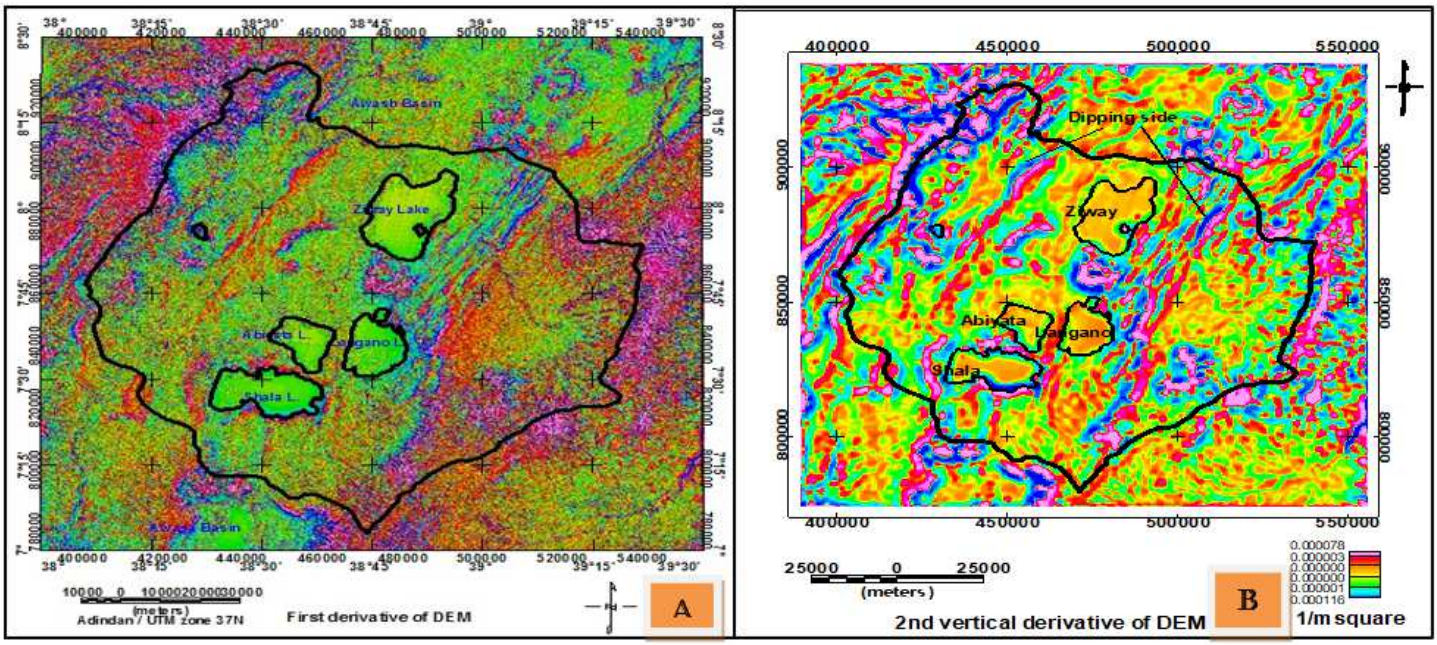

Figure 10

First vertical derivatives of topographic (DEM) data (a) Lineaments extracted from DEM using second order derivative with dip directions towards low color contrast (e.g. blue color) (b)

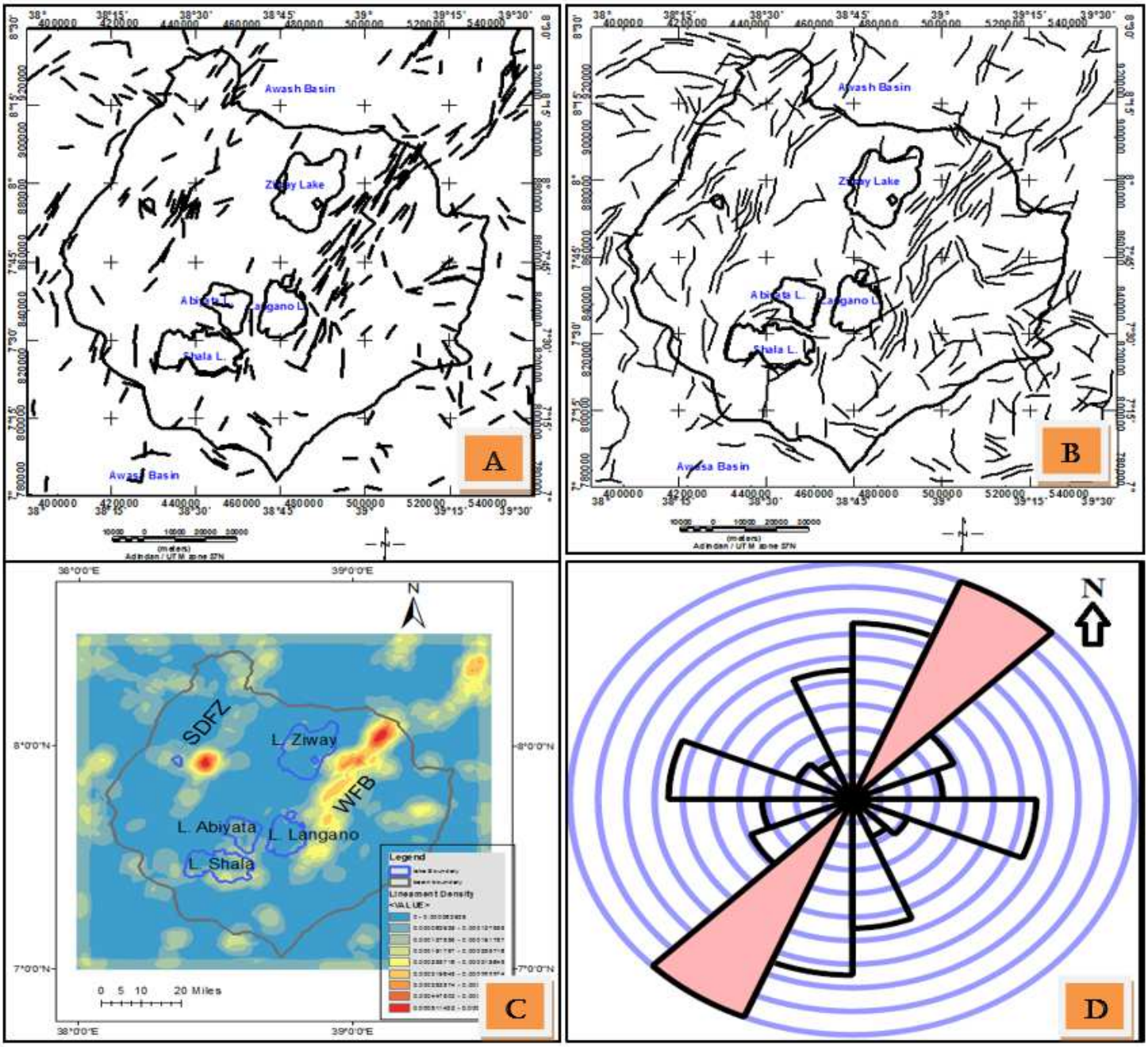

Figure 11

Automatically extracted lineaments with DEM slope gradient as an input with parameters taken from choice 1 (a); choice 2(b) and lineament density map of the study area (c) using lineaments shape file from lineaments (a) as an input. Rose diagrams showing the overall orientation (directional trend) of surface lineaments extracted from DEM (d)

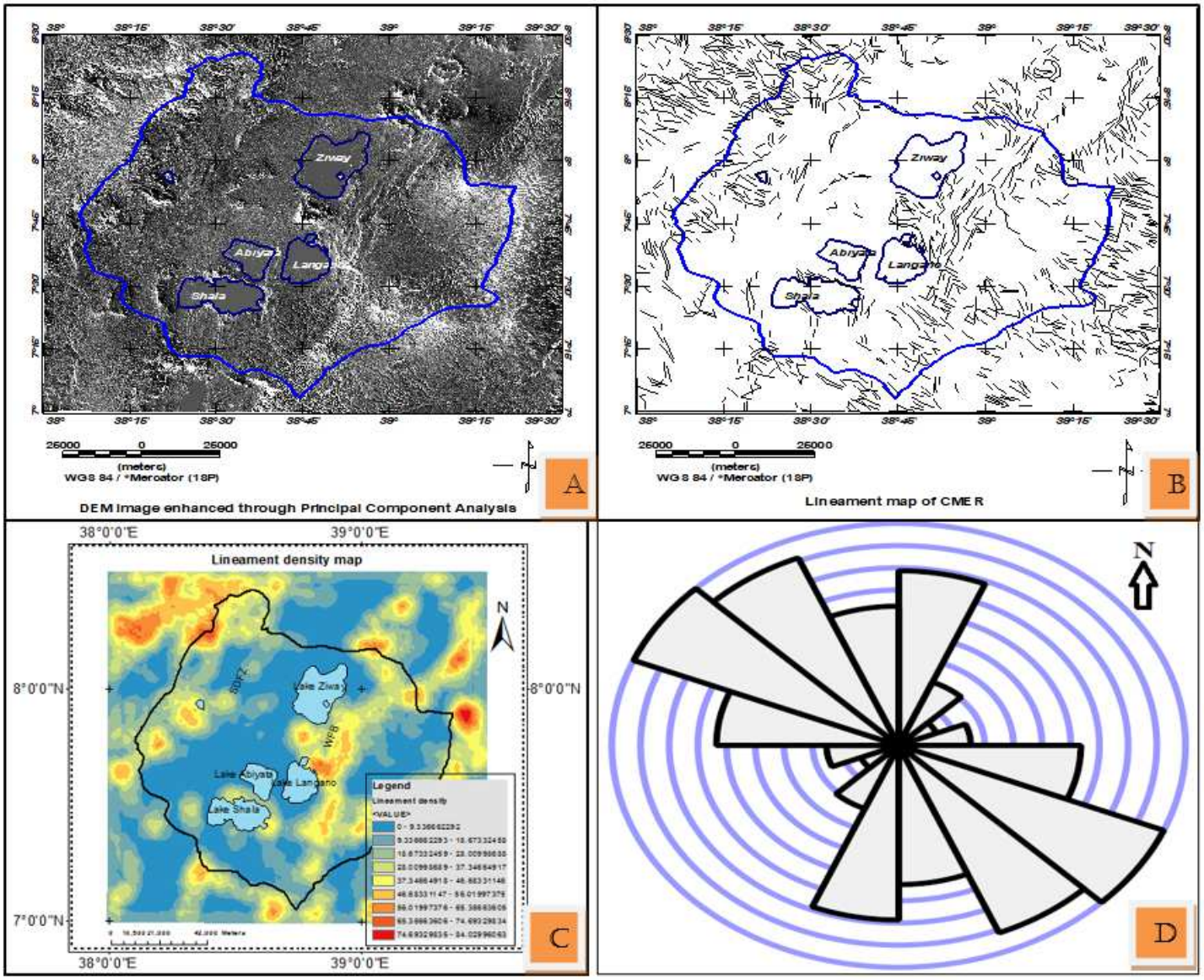

Figure 12

Enhanced DEM map using Principal Component Analysis (a) automatically extracted lineaments from DEM using PCI Geomatica software with image (a) as an input (b) Lineaments generated in (b) was exported to ArcGIS 10.3 where all processing and density map is generated and shown in (c) the Rose diagram showing dominant NW-SE and less dominant NNE-SSW trending lineaments.

Supplementary Files

This is a list of supplementary files associated with this preprint. Click to download.

- graphicalabstract2.docx